Electronic Supplementary Material (ESI) for Green Chemistry.
This journal is © The Royal Society of Chemistry 2021

Electronic Supplementary Information

Sustainable, self-cleaning, transparent, and moisture/oxygen-barrier coating for food packaging

Vu Thi Tuyet Thuy,[a,b,‡] Lam Tan Hao,[a,b,‡] Hyeonyeol Jeon,[a] Jun Mo Koo,[a] Jaeduk Park,[c] Eun Seong Lee,[c] Sung Yeon Hwang,[a,b,*] Sejin Choi,[a,*] Jeyoung Park,[a,b,*] and Dongyeop X. Oh[a,b,*]

[a]*Research Center for Bio-Based Chemistry, Korea Research Institute of Chemical Technology (KRICT), Ulsan 44429, Republic of Korea*

[b]*Advanced Materials and Chemical Engineering, University of Science and Technology (UST), Daejeon 34113, Republic of Korea.*

[c]*Department of Biomedical Chemical Engineering, The Catholic University of Korea, Bucheon-si 14662, Gyeonggi-do, Republic of Korea*

‡These authors contributed equally.

*Corresponding authors: crew75@krict.re.kr; schoi@krict.re.kr; jypark@krict.re.kr; dongyeop@krict.re.kr

Table S1. Size and surface zeta potential of nanomaterials: chitosan nanowhiskers (CsW), silica nanoparticles (SiO_2 NP), and cellulose nanofibers (CNF)

Characterization	**CsW (pH 4)**	**SiO_2 NP**	**CNF (pH 7)**
Zeta potential (mV)	+40.3	−30.0	−44.9
Aspect ratio	6.3	1.0	21
Width (nm)	42 ± 13	20–30	15 ± 3
Length (nm)	191 ± 47	20–30	209 ± 74

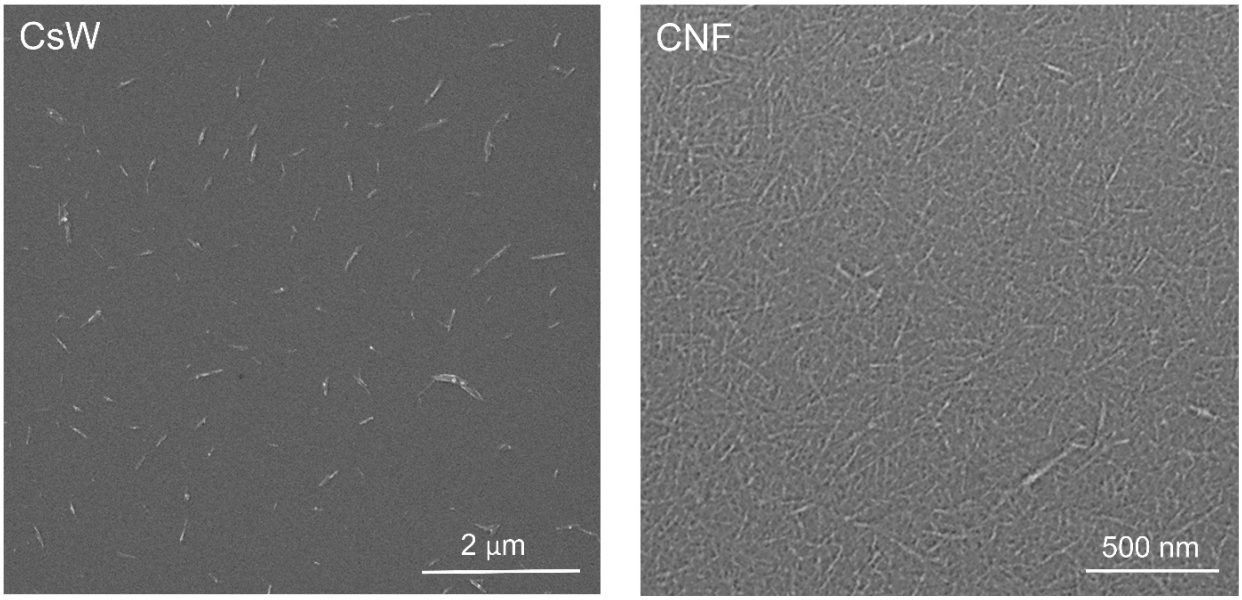

Figure S1. SEM images of CsW (left), and CNF (right).

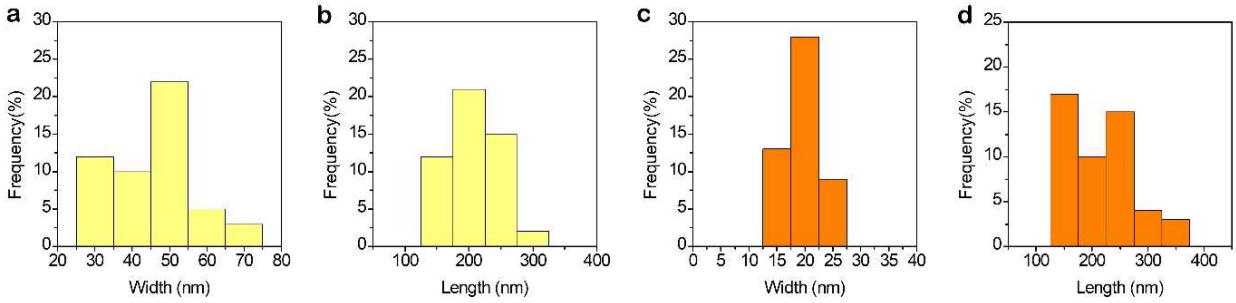

Figure S2. Size distribution of CsW: (a) width and (b) length, and CNF: (c) width, and (d) length.

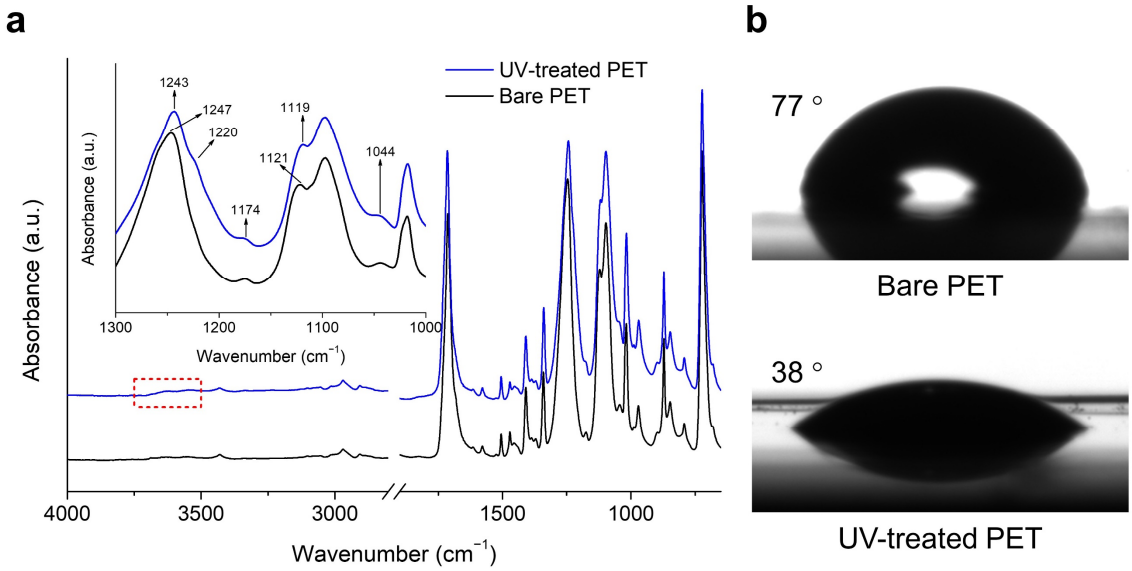

Figure S3. (a) Attenuated total reflectance-Fourier transform infrared (ATR-FTIR) spectra and (b) water contact angles of the PET film before and after irradiation with ultraviolet (UV) light. The inset of (a) is the same spectra in the 1300–1000 cm^{-1} region.

UV irradiation led to chain scission of the poly(ethylene terephthalate) (PET) film, particularly on the polar C–O bond. The ester C–O stretching signals exhibited a red shifting from 1247 to 1243 cm^{-1} and from 1121 to 1119 cm^{-1}, and a peak shouldering at 1174 and 1044 cm^{-1}, suggesting a decrease in the bond strength induced by UV irradiation. Internal C–C chain cleavage, such as in the ethylene portion also occurred, thus affecting the strength of neighbouring C–O bonds, resulting in the emergence of a shoulder at 1220 cm^{-1}. Moreover, a slight evolution of the broad OH stretching vibration in the 3500–3750 cm^{-1} region was observed in the UV-treated PET film, suggesting the generation of more hydrophilic and reactive groups such as carboxylic acid and alcohol. In addition, an increase in the hydrophilicity of the UV-treated PET film surface was verified with a twofold decrease in water contact angle from 77° to 38°.

Table S2. Coating thickness of the $(CsW/CNF)_n$ layer on PET films (GBn), OTR, and WVTR of the GBn films and the GB40-P2-O film

Sample	**$(CsW/CNF)_n$ coating thickness (µm)**	**OTR at 23 °C, 0% RH* (mL m^{-2} day^{-1})**	**WVTR at 23 °C, 0% RH* (g m^{-2} day^{-1})**
Neat PET	0 (no coating)	38.1 ± 1.40	8.50 ± 0.05
GB10	1.56 ± 0.20	26.8 ± 0.32	7.08 ± 0.67
GB20	3.50 ± 0.95	8.10 ± 1.40	4.55 ± 0.19
GB30	5.11 ± 1.10	2.45 ± 0.07	4.03 ± 0.13
GB40	7.10 ± 0.89	1.61 ± 0.01	3.67 ± 0.07
GB40-P2-O	7.10 ± 0.89	< 0.1†	1.44 ± 0.05

*RH: relative humidity; † below the limit of the OTR tester.

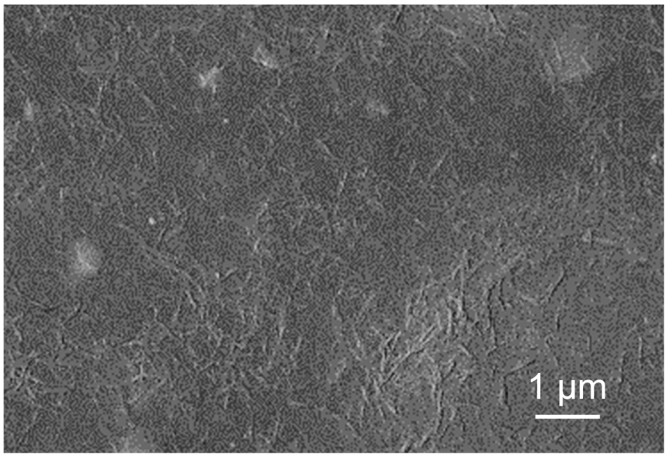

Figure S4. SEM image of the $(CsW/CnF)_{10}$-coated PET (GB10) surface showing the strongly adhered (CsW/CNF) coating that cannot be removed by finger rubbing for 50 times.

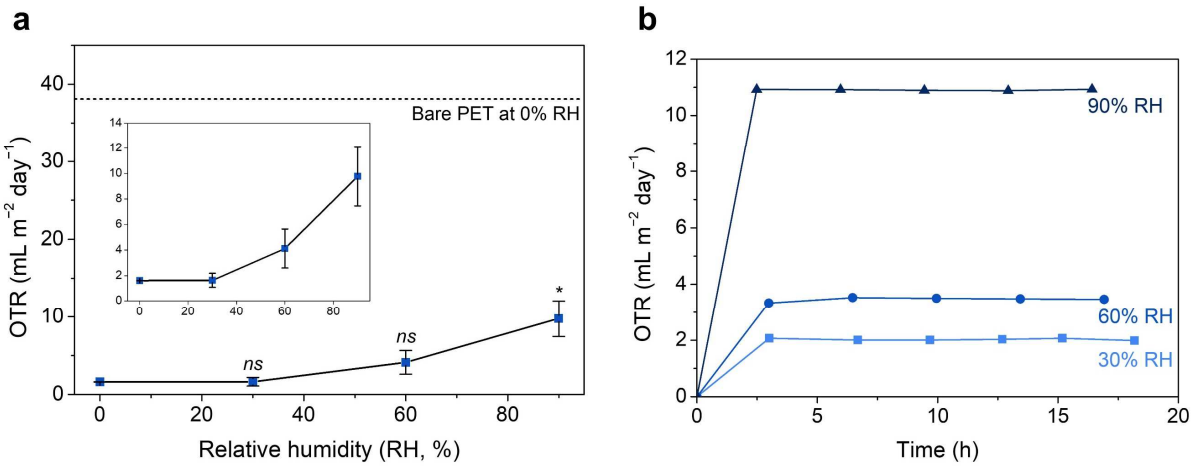

Figure S5. (a) Oxygen transmittance rate (OTR) curve of the $(CsW/CNF)_{40}$-coated PET (GB40) film as a function of the relative humidity (RH) at 23 °C. A close-up of the lower OTR region is shown in the inset. Data are expressed as the mean ± standard deviation of triplicate samples (n = 3). *ns*: non-significance, and * significant at p<0.05 compared with the 0% RH condition in the Student's t-test. (b) Stabilization of OTR readings of the GB40 film at various RH during the measurement.

Table S3. Tabular data for the OTR of the GB40 film at various relative humidity at 23 °C

Relative humidity (%)	**OTR (mL m^{-2} day^{-1})**
0	1.61 ± 0.01
30	1.63 ± 0.56
60	4.12 ± 1.53
90	9.77 ± 2.31

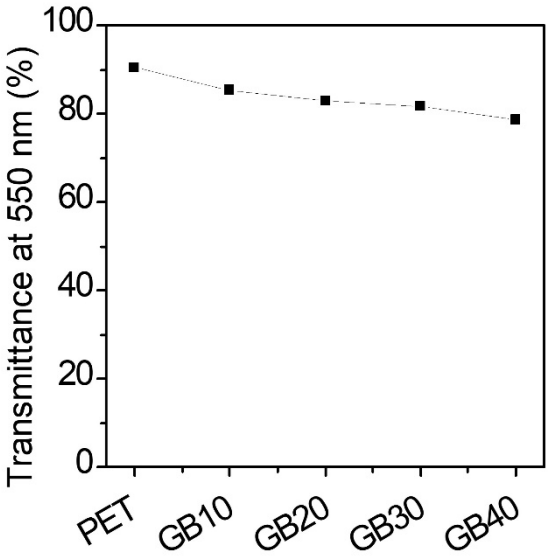

Figure S6. Transmittance at a wavelength of 550 nm of different number of bilayers of CsW/CNF coating on the PET films, with GB10, GB20, GB30, GB40 assigned to 10, 20, 30 and 40 bilayers coated on the PET films, respectively.

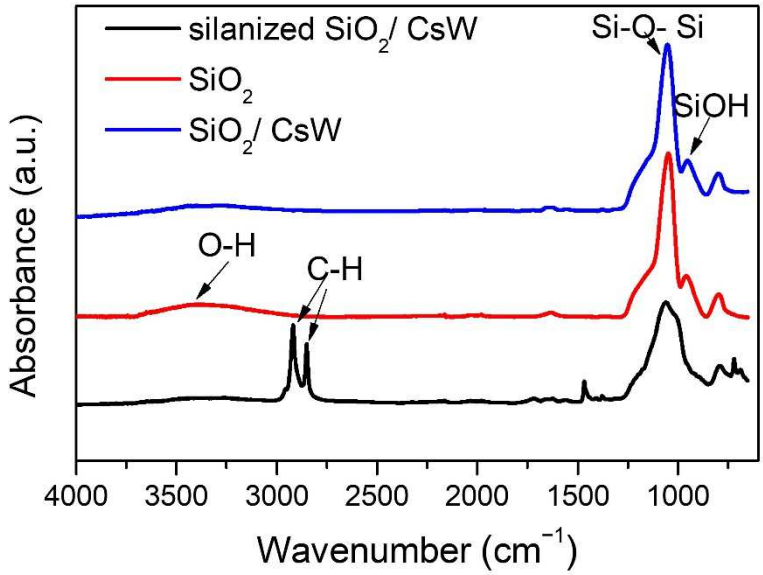

Figure S7. ATR-FTIR spectra of SiO_2 NP, and CsW/SiO_2 NP formed by layer-by-layer (LbL) deposition before and after silanization.

ATR- IR spectra revealed the stretching vibration of hydroxyl groups at 3361 cm^{-1} and bending vibration of Si–O(–H) at 958 cm^{-1} in SiO_2 NPs. The C–H (sp^3) vibrations at 2916 cm^{-1} and 2852 cm^{-1} confirmed the presence of alkyl chains in trichloro octadecyl silane. This can be attributed to the reaction between Si–Cl active bonds in the silane agents and the hydroxyl groups on the surfaces of SiO_2 NPs to form Si–O–Si bonds. Moreover, the vibration at 1460 cm^{-1} belongs to the scissoring vibration of C–H (sp^3).

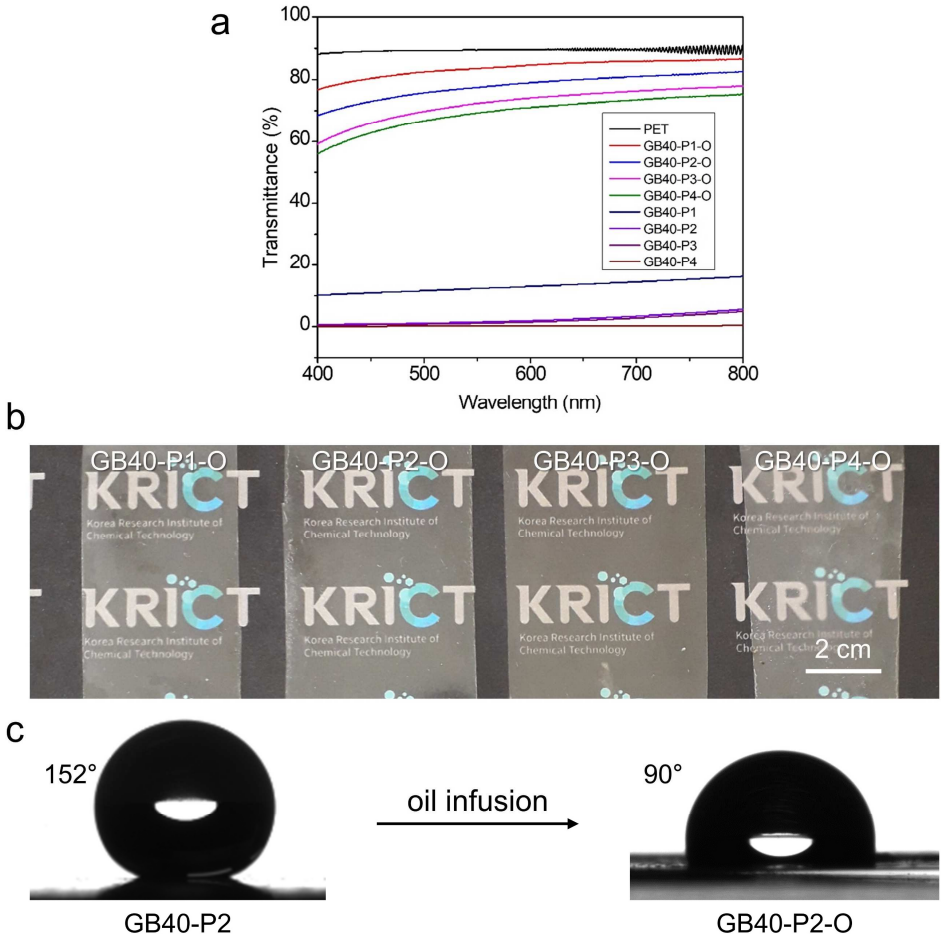

Figure S8. (a) Transmittance of different numbers of (CsW/SiO_2 NP) coating on the GB40 film before oil infusion (GB-40-Pm) and after oil infusion (GB40-Pm-O). (b) Photographs of the GB40-Pm-O films (*m* = number of P layers). (c) Representative photos of the water contact angle measurement of the P2 surface before and after the sunflower oil infusion.

The transparency of the coated films increases after oil infusion (Fig. S8a,b) owing to the presence of the lubricant oil, which reduced the reflective index between air and the coated PET interface. A higher number of bilayers of the porous P coating (*i.e.*, increased coating thickness), produce a lower transmittance. Moreover, oil infusion eliminates any surface roughness (Fig. S8c) and results in decreased contact angles of all GB-40-Pm-O samples.

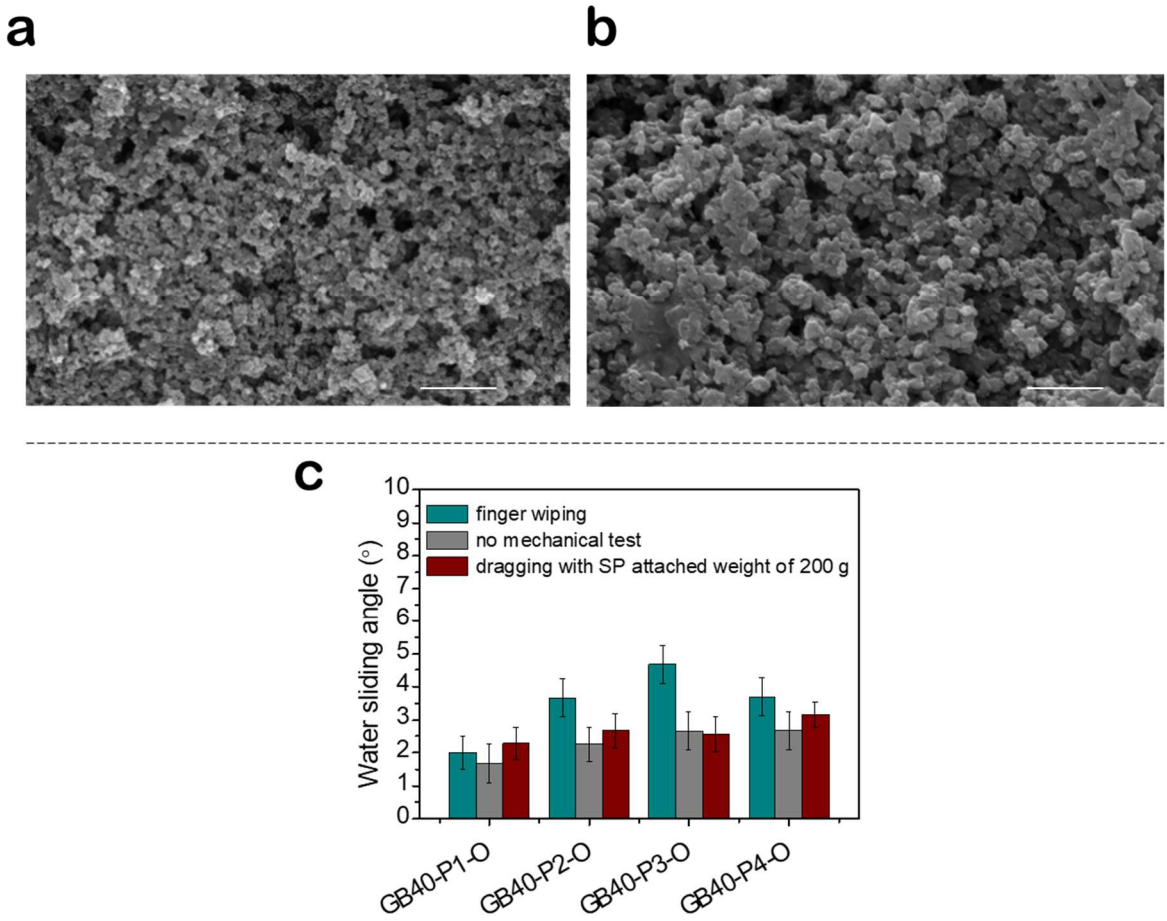

Figure S9. SEM images after evaluating the mechanical robustness of GB40-P2: (a) after manual touching, and (b) after strong wiping (scale bar: 2 µm). (c) Water sliding angle before and after mechanical testing: after strong finger wiping, and after dragging a sandpaper (SP) placed under a weight of 200 g for 1 time.

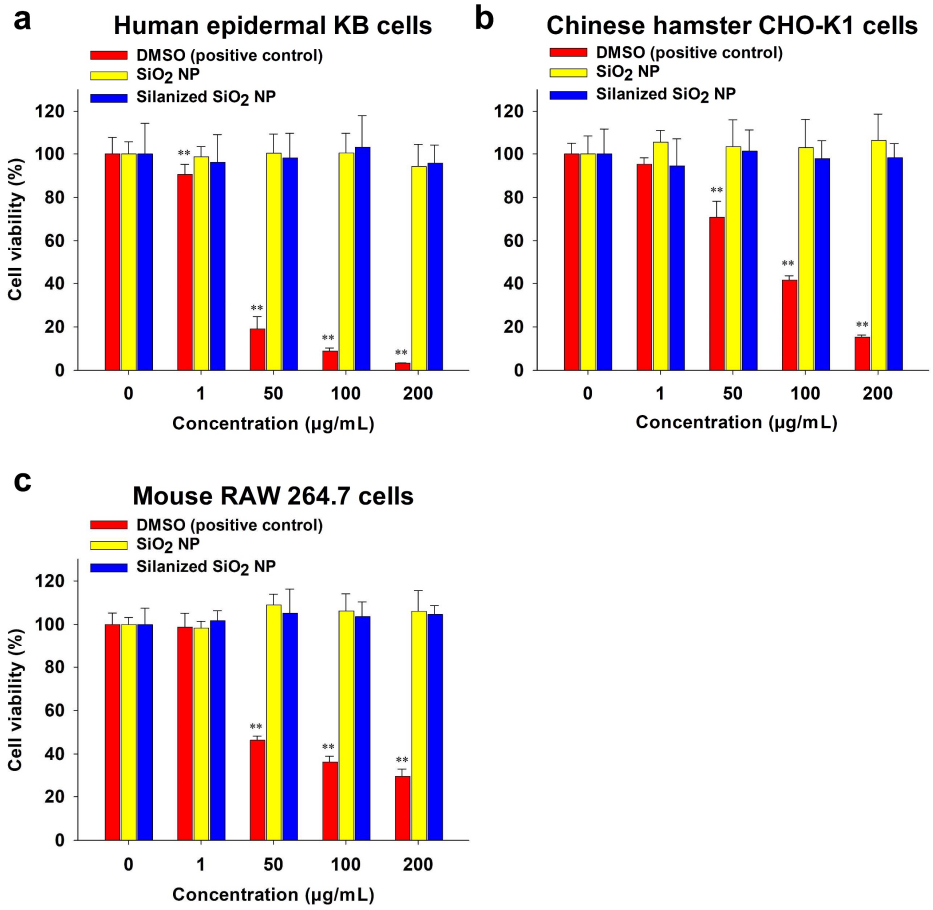

Figure S10. *In vitro* cell viability tests of the positive control (cell culture medium with 5% dimethyl sulfoxide *i.e.*, DMSO), SiO_2 NPs, and silanized SiO_2 NPs using three different types of cells: (a) human epidermal KB, (b) Chinese hamster CHO-K1, (c) mouse RAW 264.7 cells. Data are expressed as the mean ± standard deviation of quintuplicate samples (n = 5). ** p<0.01 compared with the negative control (0 μg/mL) in the Student's t-test.

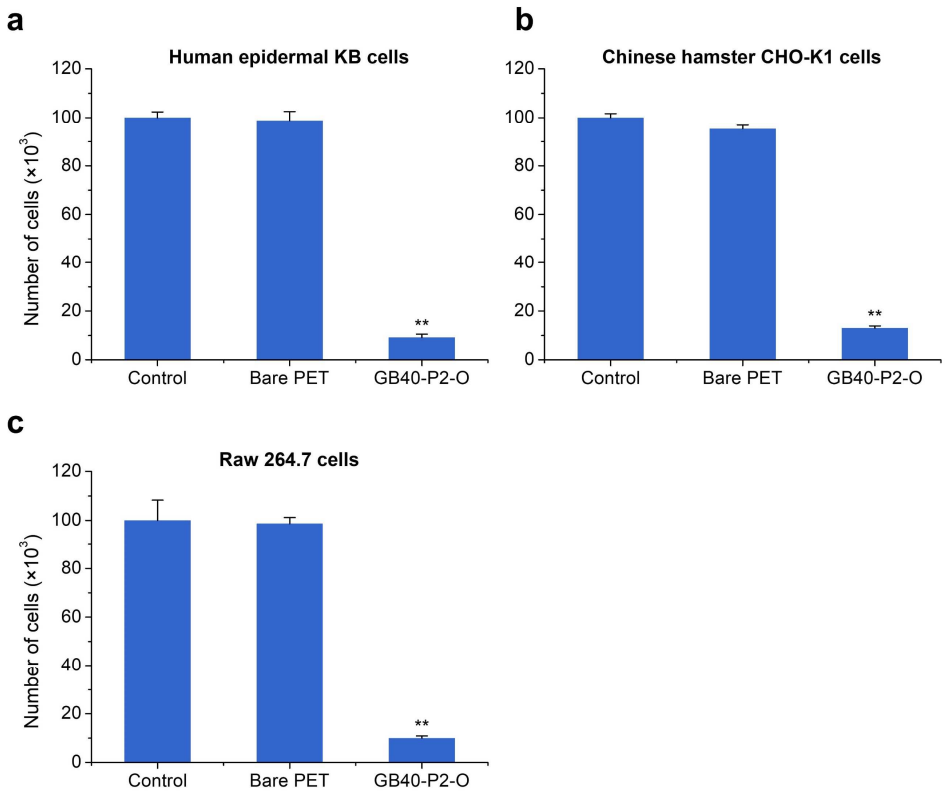

Figure S11. Quantification of the cell attachment using (a) human epidermal KB, (b) Chinese hamster CHO-K1, and (c) mouse RAW 264.7 cells on PET and GB40-P2-O films. The control is the blank culture well plate with no addition of films. Data are expressed as the mean ± standard deviation of triplicate samples (n = 3). ** p<0.01 compared with the control in Student's t-test.

Supporting Movies

Movie S1. Fabrication procedure of the functional PET films.

Movie S2. Water sliding angle of SLIPS after subjected to centrifugation at 4,000 rpm/10,000 rpm.

Movie S3. Water sliding angle of SLIPS after 1 time/10 times of dragging sandpaper attached a weight of 100 g/1 kg.

Movie S4. Stability of the infused sunflower oil against oil-absorbing potato chips.

Movie S5. Repellence ability of the GB40-P2-O film with various liquids.

As shown in Movie S5 (00:13), the GB40-P2-O film repelled some oil-containing liquids such as milk and mayonnaise, even though its porous structure was infused with sunflower oil. We suggest that the oil of the test liquids was emulsified in water and stabilized (in terms of free energy). Simultaneously, the sunflower oil efficiently interacted with the silanized (CsW/SiO_2 NP) porous structure and was also stabilized. Therefore, the oil components of the test liquid and the film were not miscible; that is, they satisfied the test liquid-lubricant immiscibility of SLIPS (*Nature*, 2011, **477**, 443–447).